

特征喷涂参数对等离子喷涂纳米 Al_2O_3 -13% TiO_2 涂层微观结构及耐磨性能的影响

贺毅, 马东林, 金玉山, 钟标钊

(西华大学 材料学院, 成都 610039)

摘要: 目的 研究等离子喷涂纳米 Al_2O_3 -13% TiO_2 的特征喷涂参数(CPSP)对涂层微观结构及耐磨性能的影响, 探索更合理的等离子喷涂工艺参数。方法 采用等离子喷涂, 在Q235钢表面制备过渡层为NiCrAl、陶瓷层为纳米 Al_2O_3 -13% TiO_2 的涂层系统。对涂层试样进行高温和常温磨损性能测试, 并对比分析喷涂粉末、涂层的微观结构和相组成。结果 纳米涂层为微观双模结构, 由部分熔化区和完全熔化区组成, 存在裂纹、孔隙等缺陷, 其主要物相为 α - Al_2O_3 , γ - Al_2O_3 和 rutile- TiO_2 。纳米涂层磨损失效的主要原因是内部板条的分层剥落和涂层表面材料的塑性变形切削。结论 随着CPSP的增大, 纳米涂层的耐磨性能增强, 且高温磨损性能较室温磨损性能为差。纳米 Al_2O_3 -13% TiO_2 涂层微观结构中部分熔化区结构和纳米晶粒的存在显著提高了涂层的耐磨性。

关键词: 等离子喷涂; 纳米 Al_2O_3 -13% TiO_2 涂层; 特征喷涂参数; 微观组织结构; 耐磨性能

中图分类号: TG174.442 **文献标识码:** A **文章编号:** 1001-3660(2015)05-0031-07

DOI: 10.16490/j.cnki.issn.1001-3660.2015.05.006

Influence of CPSP on Microstructure and Wear Property of Nanostructured Al_2O_3 -13% TiO_2 Coating Deposited by Plasma Spraying

HE Yi, MA Dong-lin, JIN Yu-shan, ZHONG Biao-zhao

(School of Materials Science and Engineering, Xihua University, Chengdu 610039, China)

ABSTRACT: **Objective** To study the influence of different critical plasma spray parameters (CPSP) on the microstructure and the wear property of nanostructured Al_2O_3 -13% TiO_2 coating deposited by plasma spraying so as to optimize the plasma spraying parameters. **Methods** Nanostructured alumina-titania coatings with NiCrAl as the transition layer and Al_2O_3 -13% TiO_2 as the ceramic layer on the surface of the Q235 steel were prepared by plasma spraying. The wear property of the coatings at room temperature and at high temperature was respectively tested, and phase constitutions and the microstructure of spraying powder and coating layer were respectively analyzed by XRD and SEM. **Results** The results showed that the nanostructured coating had a bio-model structure,

收稿日期: 2014-12-09; 修订日期: 2015-02-01

Received : 2014-12-09; Revised : 2015-02-01

基金项目: 四川省科技厅应用基础研究资金资助项目(2009JY0141); 西华大学人才培养基金资助项目(R0910105)

Fund: Supported by the Applied Basic Research Program of Science and Technology Commission Foundation of Sichuan Province(2009JY0141), and the Talent Cultivation Program of Xihua University(R0910105)

作者简介: 贺毅(1969—), 女, 重庆人, 博士, 副教授, 主要研究方向为表面工程和高性能结构材料。

Biography: HE Yi (1969—), Female, from Chongqing, Doctor, Associate professor, Research focus: surface engineering and high performance structural materials.

consisting of PM region and FM region with defects such as crack and pore. The main phases were α - Al_2O_3 , γ - Al_2O_3 and rutile- TiO_2 . Lamination and spallation of coating materials, and the plastic deformation of nanostructured coating materials were the main reasons for coating system failure during the sliding wear test. **Conclusion** With the ascending of CPSP, the wear property increased, and the wear property at room temperature was better than that at high temperature. The presence of PM region and nanocrystals in the nanostructured Al_2O_3 -13% TiO_2 coating significantly increased the wear property.

KEY WORDS: plasma spraying; nanostructured Al_2O_3 -13% TiO_2 coatings; CPSP; microstructure; wear property

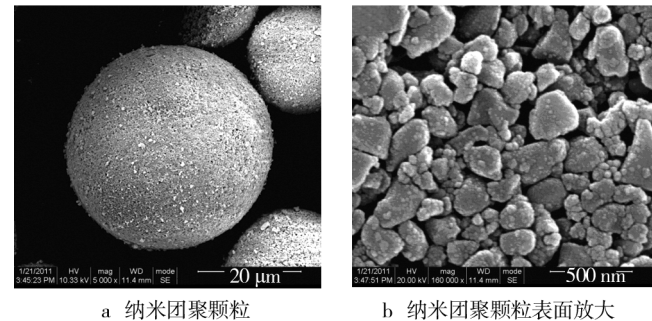
随着 21 世纪初,纳米氧化铝涂层成功应用在美军潜艇的关键部位上,人们对等离子喷涂纳米氧化铝的研究逐渐增多^[1-8]。M. Gell 等采用等离子喷涂法制备氧化铝涂层时发现^[3-5],在保持送粉、枪距、喷枪移动速度等喷涂条件不变的情况下,涂层的性能与特征喷涂参数(简称 CPSP)关系密切。CPSP 定义为: $\text{CPSP} = I \times U / Q$ (I 为电流, U 为电压, Q 为主气流量)。由公式可以看出,随着电压、电流变大,喷涂功率将显著增大;随着主气流量的降低,喷涂颗粒在等离子焰流中的停留时间将延长。从这两方面的分析可以得知,随着 CPSP 的增大,颗粒的熔化状态将发生显著变化,即较小 CPSP 参数下与较大 CPSP 参数下制备的纳米涂层在微观结构、物相组成、显微硬度、孔隙率方面将存在明显区别,进而耐磨性能受到影响。文中拟研究等离子喷涂纳米 Al_2O_3 -13% TiO_2 (13% 为质量分数,全文同)陶瓷涂层系统的常温、高温磨损失效机理,以及 CPSP 对其的影响。

1 实验

1.1 材料

基材采用 Q235 钢,尺寸为 40 mm × 20 mm × 5 mm。过渡层原料为 NiCrAl 自熔性合金粉末,粒度为 -140,+260 目,成分(以质量分数计)为:Cr 17% ~ 19%,Al 5% ~ 6.5%,Ni 74.5% ~ 78%。陶瓷喷涂原料选用 NanoxTM S2613P 纳米 Al_2O_3 -13% TiO_2 粉末,颗粒大小为 50 ~ 500 nm,成分(以质量分数计)为: $w(\text{Al}_2\text{O}_3) : w(\text{TiO}_2) = 87 : 13$, CeO_2 6% ~ 8%, ZrO_2 8% ~ 10%。

纳米 Al_2O_3 -13% TiO_2 粉末是将 Al_2O_3 , TiO_2 , ZrO_2 , CeO_2 颗粒混合均匀,经喷雾造粒、等离子体焰流处理、热处理等工序处理后制得,其微观形貌特征如图 1 所示。由图 1a 可以看出,纳米颗粒材料经团聚造粒后呈球形。图 1b 为纳米团聚颗粒表面局部放大图,可见其内部存在着一定数量的孔隙,纳米范围内的颗粒清晰可见。



a 纳米团聚颗粒 b 纳米团聚颗粒表面放大

图 1 纳米 Al_2O_3 -13% TiO_2 粉末微观形貌

Fig. 1 Micro-morphology of nanostructured Al_2O_3 -13wt.% TiO_2 powders: a) nanostructured powder; b) nanostructured powder surface

1.2 涂层制备

纳米 Al_2O_3 -13% TiO_2 涂层采用 APS-2000 型等离子喷涂系统制备,用 DPSF-2 型送粉器送粉,送粉方式为枪外径向送粉,喷枪型号为 PQ-1S。主气采用 Ar,次气选用 H₂。喷涂之前,先在基材表面喷涂厚约 50 μm 的 NiCrAl 过渡层。在喷涂距离 150 ~ 200 mm、送粉转速 6 r/min、送粉气流量 300 L/h 的条件下,按照表 1 的参数制备纳米 Al_2O_3 -13% TiO_2 涂层。

表 1 纳米 Al_2O_3 -13% TiO_2 涂层相关喷涂参数

Tab. 1 Plasma spray parameters of nanostructured Al_2O_3 -13wt.% TiO_2 coatings

| 编号 | U/V | I/A | $Q/$ | $\text{CPSP}/$ ($\text{A} \cdot \text{V}/(\text{L} \cdot \text{min}^{-1})$) |
|----|-------|-------|--------------------------------------|--|
| | | | ($\text{L} \cdot \text{min}^{-1}$) | |
| N1 | 55 | 550 | 45 | 672 |
| N2 | 55 | 600 | 45 | 733 |
| N3 | 60 | 550 | 40 | 825 |
| N4 | 60 | 600 | 40 | 900 |
| N5 | 65 | 550 | 35 | 1021 |
| N6 | 65 | 600 | 35 | 1114 |

1.3 性能测试

采用 MMU-5G 屏显式高温材料端面磨损试验机,参照国际标准 ASTM G99—04 测试纳米 Al_2O_3 -13%

TiO_2 涂层的常温、高温磨损性能。销钉材料采用热压烧结 Si_3N_4 棒料(努氏硬度为 35 GPa),其尺寸为 $\phi 5 \text{ mm} \times 15 \text{ mm}$ 。喷涂纳米 Al_2O_3 -13% TiO_2 涂层的下试样作为销盘,其尺寸为 $\phi 43 \text{ mm} \times 3 \text{ mm}$ 。分别在室温(25 °C)和高温(600 °C)下进行磨损实验,实验压力为 200 N,转速为 100 r/min,磨损时间为 30 min。试样在磨损前后,均进行超声波清洗、烘干、称量,称量仪器为 METTLER TOLEDO EL204 精密电子天平。

采用 HITACHI S3400 型扫描电镜对磨损前后的纳米 Al_2O_3 -13% TiO_2 涂层进行表面和截面观察。采用 DX2500 型 X 射线衍射仪检测纳米粉末和纳米涂层的物相组成,条件为:采用 Cu 靶 $\text{K}\alpha$ 线,管电压 40 kV,管电流 25 mA,扫描角度 $10^\circ < 2\theta < 85^\circ$,扫描速度 $0.03 (\text{ }^\circ)/\text{s}$ 。

2 结果与分析

2.1 纳米 Al_2O_3 -13% TiO_2 粉末和涂层的物相组成

经 XRD 分析(图 2)可知,纳米 Al_2O_3 -13% TiO_2 团聚颗粒的主要物相为 α - Al_2O_3 和 Anatase- TiO_2 (锐钛矿),纳米 Al_2O_3 -13% TiO_2 涂层的主要物相为 α -

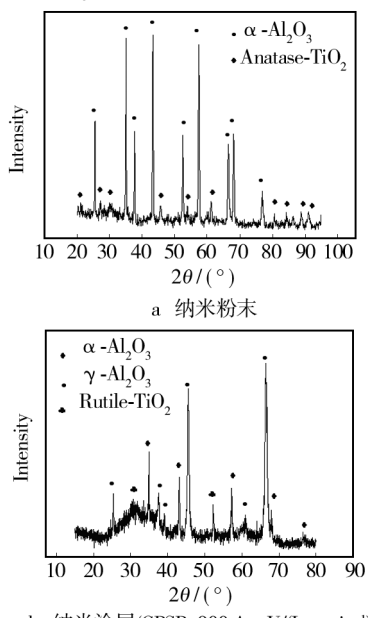


图 2 纳米 Al_2O_3 -13% TiO_2 粉末和涂层的 XRD 衍射结果

Fig. 2 XRD results of nanostructured Al_2O_3 -13wt.% TiO_2 powders and coatings: a) nanostructured Al_2O_3 -13wt.% TiO_2 powders; b) nanostructured Al_2O_3 -13wt.% TiO_2 coatings ($\text{CPSP}=900 \text{ A} \cdot \text{V}/(\text{L} \cdot \text{min}^{-1})$)

Al_2O_3 , γ - Al_2O_3 和 Rutile- TiO_2 (金红石)。等离子喷涂的加热、冷却速度极快,原料 α - Al_2O_3 在等离子焰流中快速熔化,随后极快冷却,在高的凝固速率下,在 Al_2O_3 液相/固相界面处,由于 γ - Al_2O_3 具有比 α - Al_2O_3 更低的界面能,所以 γ - Al_2O_3 优先形核并长大,因此涂层中形成了 γ - Al_2O_3 ^[7]。

2.2 纳米 Al_2O_3 -13% TiO_2 涂层的微观形貌

图 3 是纳米 Al_2O_3 -13% TiO_2 涂层的表面和截面形貌。由图 3a 可以看出,涂层表面是由完全熔化颗粒和部分熔化颗粒组成的微观双模结构(bio-model structure),喷涂材料呈“薄饼状叶片”或“花瓣状叶片”(也称板条状)平铺在基材表面。由图 3b 可以看出,涂层截面的结构同样为微观双模结构,由部分熔化区(PM)和完全熔化区(FM)组成,存在裂纹、孔隙等缺陷。

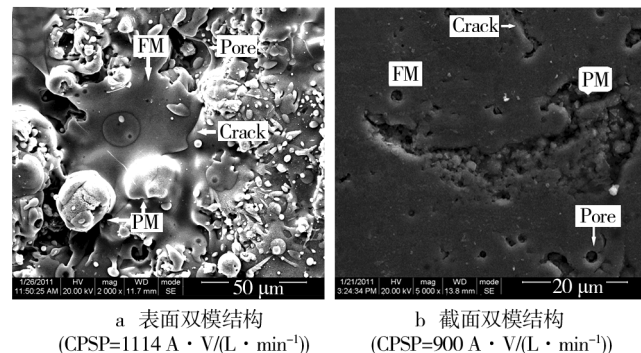


图 3 纳米 Al_2O_3 -13% TiO_2 涂层形貌

Fig. 3 Morphology of nanostructured Al_2O_3 -13wt.% TiO_2 coatings: a) bio-model structure of the surface, $\text{CPSP}=1114 \text{ A} \cdot \text{V}/(\text{L} \cdot \text{min}^{-1})$; b) bio-model structure of the cross section, $\text{CPSP}=900 \text{ A} \cdot \text{V}/(\text{L} \cdot \text{min}^{-1})$

制备纳米涂层时,由于纳米材料因其内部界面较多,对传热声子的散射较大,使得某些处于不利位置的纳米颗粒对热量的吸收更缓慢^[1],未获得足够热量的颗粒将形成表面的部分熔化颗粒,处于有利位置的纳米颗粒对热量吸收充分而形成完全熔化颗粒,最后形成涂层内部的完全熔化区和部分熔化区^[3-5]。熔化颗粒喷射到基材表面后,冷却速度极快,可达 10^5 K/s ,快速的冷却收缩易形成裂纹和孔洞。

2.3 纳米 Al_2O_3 -13% TiO_2 涂层磨损性能及 CPSP 的影响

在不同 CPSP 参数下制备的纳米 Al_2O_3 -13% TiO_2 涂层厚度均控制在 200 μm 左右,相同 CPSP 参数下

的涂层质量基本一致。在室温(25 °C)和高温(600 °C)下,纳米涂层的磨损失重数据及其与CPSP的关系见图4。随着CPSP的增大,纳米涂层的磨损失重减少,当CPSP=1114 A·V/(L·min)时,制备的纳米涂层室温、高温磨损性能最好。相同CPSP参数下制备的涂层厚度和质量相近,其室温磨损失重均少于高温磨损失重。

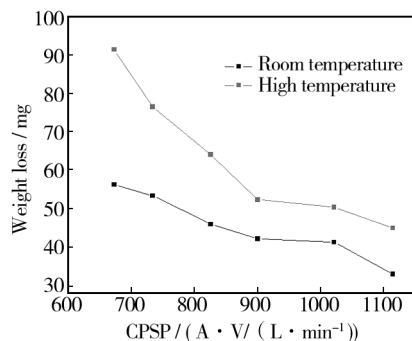


图4 室温和高温下纳米 Al_2O_3 -13% TiO_2 涂层磨损失重数据及其与CPSP的关系

Fig. 4 Wear weight loss of nanostructured Al_2O_3 -13wt.% TiO_2 coatings at room temperature (25 °C) and at high temperature (600 °C) and its relationship with CPSP

图5为涂层经常温磨损后的表面形貌。如图5a所示,磨损表面分为光滑区域和粗糙区域。在粗糙区域内部,存在沿层与层界面处的剥离和沿涂层内部晶界的断裂剥离,如图5b所示。在光滑区域表面,有纵横交错的裂纹和白色氧化物颗粒,如图5c所示。在CPSP=900 A·V/(L·min)条件下制备的涂层,磨损表面光滑区域的比例有所升高,表面有涂层材料的偶然拔出,如图5d所示。图5e为CPSP=1114 A·V/(L·min)条件下制备的涂层的磨损形貌,可见磨损变得轻微,磨痕表面几乎只由光滑区域组成。存在的凹坑是在磨损初期,凸起的颗粒被拔出而产生的,不是磨损失效的主要原因。对图5e的光滑区域进一步放大,如图5f所示,光滑区域呈现出“鱼鳞”形貌,“鱼鳞”表面有大量微观裂纹和氧化物颗粒存在。光滑区域的“鱼鳞”形貌说明,纳米涂层在磨损过程中发生了塑性变形,塑性变形区域在横向拉应力和纵向压应力的作用下,生成疲劳裂纹并分层剥落。对比纳米涂层的室温磨损失重数据及磨损表面形貌可知,随着CPSP增大,涂层磨损失重减少,磨损表面光滑区域增大,表明涂层的耐磨损性有所提高^[9-18]。涂层中存在的部分熔化区和纳米晶粒的强化作用有利于提高涂层的耐磨损性。

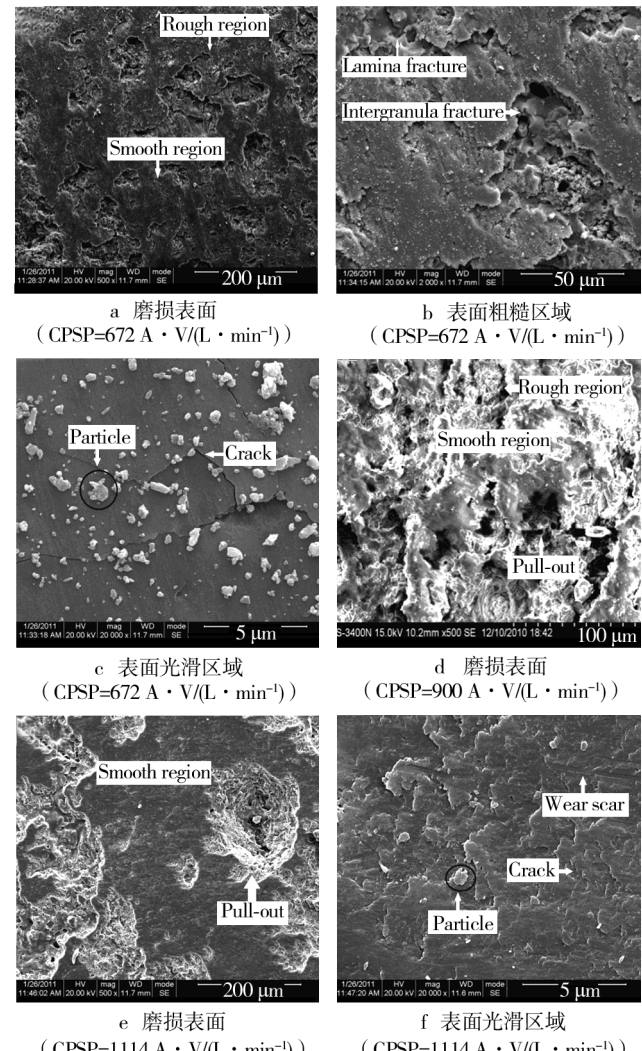


图5 不同CPSP条件下所制备涂层的室温磨损表面

Fig. 5 Wear surface of nanostructured Al_2O_3 -13wt.% TiO_2 coatings at room temperature at different CPSP; a) wear surface (CPSP=672 A·V/(L·min⁻¹)); b) rough region (CPSP=672 A·V/(L·min⁻¹)); c) smooth region (CPSP=672 A·V/(L·min⁻¹)); d) wear surface (CPSP=900 A·V/(L·min⁻¹)); e) wear surface (CPSP=1114 A·V/(L·min⁻¹)); f) smooth region (CPSP=1114 A·V/(L·min⁻¹))

图6为涂层经高温磨损后的形貌。如图6a所示,CPSP=672 A·V/(L·min)条件下制备的涂层磨损表面由光滑区和粗糙区组成,与室温磨损形貌相比,其光滑区有所减小,磨损更严重,这与纳米材料的颗粒细、界面较多致使其高温性能不理想有关。进一步放大观察光滑区,如图6b所示,可见表面存在因涂层材料分层剥落形成的粗糙区域,裂纹在光滑区表面形成,并且有白色的磨屑颗粒残留在光滑区域。CPSP=900 A·V/(L·min)条件下制得的纳米涂层

经高温磨损后,表面存在磨屑颗粒(图6c中的白色颗粒状物质),磨损表面同样由粗糙区和光滑区组成,相比于6b图,其光滑区增大;同时,在光滑区未见大量粗糙区域,只有少量的涂层材料被拔出,裂纹较少。在 $\text{CPSP}=1114 \text{ A} \cdot \text{V}/(\text{L} \cdot \text{min})$)条件下制得的纳米涂层经高温磨损后,光滑区域进一步增大,如图6e所示,并且光滑区域表面未见大量涂层材料剥落,但可观察到涂层材料沿其内部晶界断裂剥离留下的痕迹和少量裂纹。

对比室温和高温磨损后的磨屑,见图7。如图7a所示,室温磨屑的尺寸较小,在几微米至十微米之间,

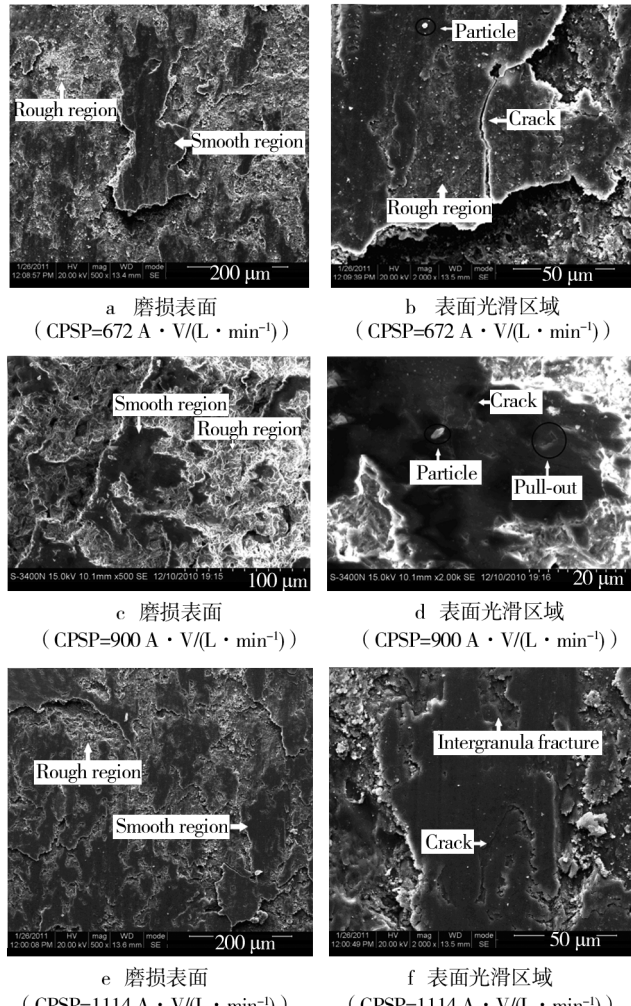


图6 不同CPSP条件下所制备涂层的高温磨损表面

Fig. 6 Wear surface of nanostructured Al_2O_3 -13wt.% TiO_2 coatings at high temperature at different CPSP: a) wear surface ($\text{CPSP}=672 \text{ A} \cdot \text{V}/(\text{L} \cdot \text{min}^{-1})$); b) smooth region ($\text{CPSP}=672 \text{ A} \cdot \text{V}/(\text{L} \cdot \text{min}^{-1})$); c) wear surface ($\text{CPSP}=900 \text{ A} \cdot \text{V}/(\text{L} \cdot \text{min}^{-1})$); d) smooth region ($\text{CPSP}=900 \text{ A} \cdot \text{V}/(\text{L} \cdot \text{min}^{-1})$); e) wear surface ($\text{CPSP}=1114 \text{ A} \cdot \text{V}/(\text{L} \cdot \text{min}^{-1})$); f) smooth region ($\text{CPSP}=1114 \text{ A} \cdot \text{V}/(\text{L} \cdot \text{min}^{-1})$)

存在涂层材料沿晶界断裂而生成的磨屑。如图7b所示,高温磨屑的大小为10~50 μm,存在表面光滑区域涂层材料的整体剥离磨屑,甚至涂层材料多层同时剥离后形成的大块磨屑。这表明高温磨损时,涂层材料的分层剥离更为严重,热应力加剧了涂层材料的磨损。

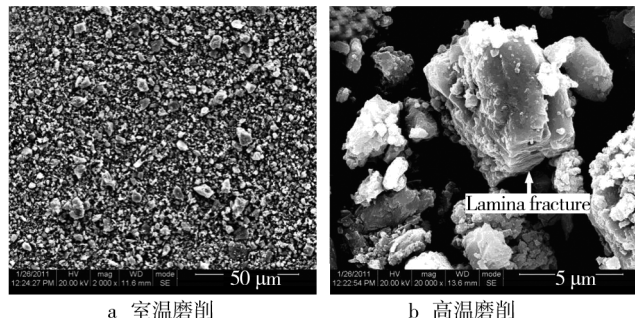


图7 涂层磨屑形貌($\text{CPSP}=900 \text{ A} \cdot \text{V}/(\text{L} \cdot \text{min}^{-1})$)

Fig. 7 Wear debris of nanostructured Al_2O_3 -13wt.% TiO_2 coatings ($\text{CPSP}=900 \text{ A} \cdot \text{V}/(\text{L} \cdot \text{min}^{-1})$): a) wear debris at room temperature; b) wear debris at high temperature

对比纳米涂层的磨损失重数据(图4)可知,随着CPSP增大,涂层在室温和高温下均更加耐磨。纳米涂层的磨损失效主要源于涂层内部板条(图3a中的FM区和图7b箭头所指处)的分层剥落和涂层表面材料的塑性变形切削。滑动磨损时,涂层内部的裂纹扩展延伸,使得板条分层剥落;涂层中预先存在的孔隙和微裂纹加速了板条的分层剥落,形成磨损表面的粗糙区域。剥落的 Al_2O_3 -13% TiO_2 颗粒存在于摩擦副间,形成三体磨损,对两个摩擦副都产生磨粒切削^[7],从而形成磨损表面的光滑区域。磨损表面的光滑区较粗糙区多,其磨损失重较少,因此涂层的耐磨性提高^[9-18]。涂层中部分熔化区的硬度低于完全熔化区,塑韧性较好^[19-21]。但在一些完全熔化区中,由于纳米晶粒的强化作用,涂层材料的塑韧性有一定程度的提高,塑性变形切削的速度减慢,故显著提高了涂层的耐磨性。

综上,随着CPSP的增大,喷涂材料颗粒的熔化状态将会更好^[5-6,22-23],板条间的结合力增大,板条结合更加牢固而不易分层剥落,也使涂层磨损表面中粗糙区域的比例减少;涂层内部的微观裂纹和孔隙数量显著降低^[3-5],减少了裂纹萌生源;部分熔化颗粒熔化加剧^[1-4,8,19,24],烧结得更加致密,塑性变形切削的速度更慢,减缓了涂层的磨损失效;这些都有助于提高涂层的耐磨性。纳米涂层随着磨损试验温度的升

高,磨损加剧。在较高温度下,由于热应力加剧,涂层内部更易萌生裂纹,且裂纹的扩展速度增加,导致涂层材料大块剥离,磨损性能降低;此外,温度升高使得晶界的强度降低,导致磨损表面的塑性变形光滑区域内部有少许涂层材料剥离;如此,便加剧了涂层的磨损失重,使得涂层的耐磨性能降低。

3 结论

- 1) 纳米 Al_2O_3 -13% TiO_2 涂层的主要物相为 α - Al_2O_3 , γ - Al_2O_3 和 Rutile- TiO_2 (金红石)。
- 2) 纳米 Al_2O_3 -13% TiO_2 涂层截面和表面是由完全熔化区(完全熔化颗粒)、部分熔化区(部分熔化颗粒)及未熔颗粒组成的微观双模结构,存在孔洞、裂纹等缺陷。
- 3) 随着 CPSP 的增大,纳米 Al_2O_3 -13% TiO_2 涂层的磨损失重减少;同时,涂层在高温下的磨损失重大于在室温下的磨损失重。纳米涂层的磨损失效主要源于涂层内部板条的分层剥落和涂层表面材料的塑性变形切削,涂层中存在的部分熔化区结构和纳米晶粒的强化作用可显著提高涂层的耐磨性。

参考文献

- [1] PAWLOWSKI Lech. Finely Grained Nanometric and Submicrometric Coatings by Thermal Spraying: A Review [J]. Surface & Coatings Technology, 2008, 202:4318—4328.
- [2] GOBERMAN D, SOHN Y H, SHAW L, et al. Microstructure Development of Al_2O_3 -13wt.% TiO_2 Plasma Sprayed Coatings Derived from Nanocrystalline Powders[J]. Acta Materialia, 2002, 50:1141—1152.
- [3] JORDAN E H, GELL M, SOHN Y H, et al. Fabrication and Evaluation of Plasma Sprayed Nanostructured Alumina-Titania Coatings with Superior Properties[J]. Mater Sci Eng A, 2001, 301:80—89.
- [4] GELL M, JORDAN E H, SOHN Y H, et al. Development and Implementation of Plasma Sprayed Nanostructured Ceramic Coatings[J]. Surface and Coatings Technology, 2001, 146/147:48—54.
- [5] SONG Eunpil , AHN Jeehoon , LEE Sunghak, et al. Effects of Critical Plasma Spray Parameter and Spray Distance on Wear Resistance of Al_2O_3 -8wt. % TiO_2 Coatings Plasma-sprayed with Nanopowders[J]. Surface & Coatings Technology, 2008, 202 :3625—3632.
- [6] SONG Eunpil, AHN Jeehoon, LEE Sunghak, et al. Microstructure and Wear Resistance of Nanostructured Al_2O_3 -8wt. % TiO_2 Coatings Plasma-sprayed with Nanopowders [J]. Surface & Coatings Technology, 2006, 201:1309—1315.
- [7] 张建新. 等离子喷涂纳米结构 Al_2O_3 -13wt.% TiO_2 涂层组织及性能研究[D]. 天津:河北工业大学, 2007. ZHANG Jian-xin. Study of the Microstructure and Properties of the Plasma-sprayed Nanostructured Al_2O_3 -13wt.% TiO_2 Coating [D]. Tianjin: Hebei University of Technology, 2007.
- [8] SHAW Leon L, GOBERMAN Daniel, REN Rui-ming, et al. The Dependency of Microstructure and Properties of Nanostructured Coatings on Plasma Spray Conditions [J]. Surface and Coatings Technology, 2000, 130:1—8.
- [9] SINGH Vinaypratap, SIL Anjan, JAYAGANTHAN R. A Study on Sliding and Erosive Wear Behaviour of Atmospheric Plasma Sprayed Conventional and Nanostructured Alumina Coatings[J]. Materials and Design, 2011, 32:584—591.
- [10] WANG You, JIANG Stephen, WANG Mei-dong, et al. Abrasive Wear Characteristics of Plasma Sprayed Nanostructured Alumina/Titania Coatings[J]. Wear, 2000, 237:176—185.
- [11] WANG Byoungchulh, LEE Sunghak, AHN Jeehoon. Correlation of Microstructure and Wear Resistance of Molybdenum Blend Coatings Fabricated by Atmospheric Plasma Spraying [J]. Materials Science and Engineering, 2004, A366:152—163.
- [12] LIN Xin-hua, ZENG Yi, DING Chuan-xian, et al. Effects of Temperature on Tribological Properties of Nanostructured and Conventional Al_2O_3 -3wt.% TiO_2 Coatings [J]. Wear, 2004, 256:1018—1025.
- [13] RAMAZANI M, KHALIL-ALLAFI J, MOZAFFARINIA R. Grindability Evaluation and Fatigue and Wear Behavior of Conventional and Nanostructured Al_2O_3 -13wt.% TiO_2 Air Plasma Sprayed Coatings [J]. Journal of Thermal Spray Technology, 2010, 19:611—616.
- [14] KESHRI Anup Kumar, SINGH Virendra, HUANG Jun, et al. Intermediate Temperature Tribological Behavior of Carbon Nanotube Reinforced Plasma Sprayed Aluminum Oxide Coating[J]. Surface & Coatings Technology, 2010, 204: 1847—1855.
- [15] TIAN Wei, WANG You, ZHANG Tao, et al. Sliding Wear and Electrochemical Corrosion Behavior of Plasma Sprayed Nanocomposite Al_2O_3 -13% TiO_2 Coatings [J]. Materials Chemistry and Physics, 2009, 118:37—45.
- [16] TIAN W, WANG Y, YANG Y. Three Body Abrasive Wear Characteristics of Plasma Sprayed Conventional and Nanostructured Al_2O_3 -13% TiO_2 Coatings [J]. Tribology International, 2010, 43:876—881.
- [17] CHEN Huang, ZHANG Ye-fan, DING Chuan-xian. Tribolo-

- gical Properties of Nanostructured Zirconia Coatings Deposited by Plasma Spraying [J]. Wear, 2002, 253: 885—893.
- [18] RICOA A, RODRIGUEZ J, OTERO E, et al. Wear Behaviour of Nanostructured Alumina-Titania Coatings Deposited by Atmospheric Plasma Spray [J]. Wear, 2009, 267: 1191—1197.
- [19] LUO Hong, GOBERMAN Daniel, SHAW Leon, et al. Indentation Fracture Behavior of Plasma-sprayed Nanostructured Al_2O_3 /13wt.% TiO_2 Coatings [J]. Materials Science and Engineering A, 2003, 346: 237—245.
- [20] BANSAL Pavitra, PADTURE Nitin, VASILIEV Alexandre. Improved Interfacial Mechanical Properties of Al_2O_3 -13wt.% TiO_2 Plasma-sprayed Coatings Derived from Nanocrystalline Powders [J]. Acta Materialia, 2003, 51: 2959—2970.
- [21] TIAN Wei, WANG You, YANG Yong, et al. Toughening and
- (上接第4页)
- [2] LI Chang-jiu, OHMORI A. Relationship between the Microstructure and Properties of Thermally Sprayed Deposits [J]. Thermal Spray Technology, 2002, 11: 365—374.
- [3] LI Chang-jiu, OHMORI A. Relationship between Particle Erosion and Lamellar Microstructure for Plasma-sprayed Alumina Coatings [J]. Wear, 2006, 260: 1166—1172.
- [4] WANG Wei-ze, XUAN Fu-zhen, LIANG Jia-chun. Effect of Substrate Temperature on the Properties and Dissolution of Plasma Spraying [J]. Thermal Spray Technology, 2012, 21(5): 908—916.
- [5] CERNUSCHI F, LORENZONI L, CAPELLI S, et al. Solid Particle Erosion of Thermal Spray and Physical Vapour Deposition Thermal Barrier Coatings [J]. Wear, 2011, 271: 2909—2918.
- [6] SPENCER K, ZHANG Ming-xing. The Use of Kinetic Metalization to Form Intermetallic Reinforced Composited Coatings by Post-spray Heat Treatment [J]. Surface and Coatings Technology, 2009, 203(20/21): 3019—3025.
- [7] GOTO Y, TSUGE A. Mechanical Properties of Unidirectionally Oriented SiC Whisker Reinforced Si_3N_4 Fabricated by Extrusion and Hot Pressed [J]. American Ceramic Society, 1993, 76: 1420—1424.
- [8] WANG Chang-an. The Effect of Whisker Orientation in SiC Whisker-reinforced Si_3N_4 Ceramic Matrix Composites [J]. European Ceramic Society, 1999, 19: 1903—1909.
- [9] SUZUKI T S, SAKKA Y, KITAZAWA K. Preferred Orientation of the Texture in the SiC Whisker-dispersed Al_2O_3 Ceramics by Slip Casting in a High Magnetic Field [J]. The Ceramic Society of Japan, 2001, 109: 886—891.
- [10] 姚奎毅, 郭英奎. SiC 晶须在高压静电场作用下單向排列

- Strengthening Mechanism of Plasma Sprayed Nanostructured Al_2O_3 -13wt.% TiO_2 Coatings [J]. Surface & Coatings Technology, 2009, 204: 642—649.
- [22] YUGESWARAN S, SELVARAJAN V, SEO D, et al. Effect of Critical Plasma Spray Parameter on Properties of Hollow Cathode Plasma Sprayed Alumina Coatings [J]. Surface & Coatings Technology, 2008, 203: 129—136.
- [23] YUGESWARAN S. Influence of Critical Plasma Spraying Parameter (CPSP) on Plasma Sprayed Alumina-Titania Composite Coatings [J]. Ceram, 2009, 10: 1016—1022.
- [24] WANG Dong-sheng, TIAN Zong-jun, SHEN Li-da, et al. Microstructural Characteristics and Formation Mechanism of Al_2O_3 -13wt.% TiO_2 Coatings Plasma-sprayed with Nanostructured Agglomerated Powders [J]. Surface & Coatings Technology, 2009, 203: 1298—1303.
- 的研究 [J]. 机械工程材料, 1997, 21(3): 19—20.
- YAO Kui-yi, GUO Ying-kui. Study of One-directional Arrangement of SiC Whiskers under High Voltage Electrostatic Field [J]. Materials for Mechanical Engineering, 1997, 21(3): 19—20.
- [11] MOREAU C, CIELO P, LAMONTAGNE M, et al. Temperature Evolution of Plasma-sprayed Niobium Particles Impacting on a Substrate [J]. Surface and Coatings Technology, 1991, 46: 173—187.
- [12] KURODA S, CLYNE T W. The Quenching Stress in Thermally Sprayed Coatings [J]. Thin Solid Films, 1991, 200: 49—66.
- [13] 李长久, 李京龙. 等离子喷涂熔滴扁平过程数值模拟 [J]. 航空制造技术, 1999, 11(5): 57—59, 62.
- LI Chang-jiu, LI Jing-long. Numerical Simulations of Droplet Flattening in Plasma Spraying [J]. Aviation Manufacturing Technology, 1999, 11(5): 57—59, 62.
- [14] BERTAGNOLLI M, MARCHESE M, JACUCCI G. Modeling of Particles Impacting on a Rigid Substrate under Plasma Spraying Conditions [J]. Thermal Spray Technology, 1995, 4(1): 41—49.
- [15] TRAPAGA G, MATTHYS E F, VALENCIA J J. Fluid Flow, Heat Transfer and Solidification of Molten Metal Droplets Impinging on Substrates: Comparison of Numerical and Experimental Result [J]. Metall Trans B, 1992, 23B: 701—718.
- [16] YAMAGUQI. Forming of Product Enhanced by Fiber in Controlled Direction [C]// Proceedings of the 1997 Annual Conference on Precision Engineering. Braunschweig: [s. n.], 1997: 210.